Charge transport in anodic TiO_2 nanotubes studied by terahertz spectroscopy

Milos Krbal[1], Jiri Kucharik[2], Hanna Sopha[1], Hynek Nemec[2] and Jan M. Macak[1,*]

[1] Center of Materials and Nanotechnologies, Faculty of Chemical Technology, University of Pardubice, Nam. Cs. Legii 565, 53002 Pardubice, Czech Republic

[2] Institute of Physics, Academy of Sciences of the Czech Republic, Na Slovance 2, 18221 Prague 8, Czech Republic

Keywords TiO_2 nanotubes, charge transport, traps, THz spectroscopy.

* Corresponding author: e-mail jan.macak@upce.cz, Phone: +420 466 037 401

We report on the photoelectrochemical and terahertz measurements, of the charge transport properties of 1 μm thick self-organized TiO_2 nanotube layers, prepared by the anodization of titanium. We provide evidence regarding the complexity of electron transport, and dynamics in the nanotubes. Shortly after photoexcitation, charge mobilites in amorphous and crystalline nanotubes are similar, but still lower compared to the bulk anatase. The mobility subsequently decreases due to trapping-detrapping processes. The recombination rate in anatase nanotubes is much slower than in the amorphous ones, enabling the material to reach an internal photon to electron conversion efficiency exceeding 60 %.

1 Introduction Self-organized TiO_2 nanotube layers possess a unique 1D nanostructure, with many intriguing properties [1,2]. Within the past 11 years, several different generations of nanotube layers were developed, providing a range of various aspect ratios and geometries. Due to their semiconductive nature, high surface area, anticipated uni-directional electron transport along their walls, and also due to the ability to be prepared on transparent conducting glasses, they have been of interest as anodes in dye-sensitized solar cells [3-5], and perovskite solar cells [6-8]. While there is a substantial knowledge about the photoresponse of the nanotubes upon UV and VIS light illumination [9-11], rather scarce information on the underlying charge transport properties have been obtained until now.

Terahertz (THz) response and charge transport properties, are closely related with the structure and architecture of the TiO_2 nanotubes. For example, a band-like transport in TiO_2 nanotube layers was observed by Wehrenfennig et al. [12], with the electron mobility comparable to that in TiO_2 nanoparticulate layers. The free electron lifetimes in these nanotubes were of the order of tens of picoseconds, which is surprisingly shorter than the electron lifetimes in films of TiO_2 nanoparticles [12]. A qualitatively different behaviour was reported by Richter and Schmuttenmaer [13] in Ru-N3-sensitized TiO_2 nanotubes: the THz response was dominated by excitons at trap states, while the charge transport was strongly suppressed. These nanotube layers were also too thick (over 40 μm) for employment in dye-sensitized or perovskite solar cells, where typically TiO_2 layers with thickness on the order of few microns and several hundreds of nanometers, respectively, are employed [3-8].

In this paper, we analyse the photoelectrochemical and THz response of 1 μm thick anodic TiO_2 nanotubular layers in the amorphous and anatase state, without any other modification. This allows us to provide a detailed description of charge transport in the nanotubes that are of particular interest to applications such as perovskite solar cells [6-8] and many other applications.

2 Results and discussion

Figure 1 shows SEM images (obtained by FE-SEM JEOL JSM 7500F) of the self-organized TiO_2 nanotube layer used in this work. The inner diameter and the length of nanotubes (64 ± 8 nm and 1.0 ± 0.1 μm, respectively) were evaluated by statistical analyses of the SEM images from the top views (Fig. 1a), and from the cross-sections of the nanotubes (Fig. 1b). Cleaning of Ti foils, their anodization, and cleaning of the anodized nanotubes was carried in distinct steps published previously [14]. A glycerol based electrolyte containing 0.27 M NH_4F and 10 vol.% H_2O was used for anodization of Ti foils at 20 V (achieved with a sweep rate of 1 V/s) for 100 min. In order to convert amorphous nanotubes to nanotubes with a defined anatase structure, samples were annealed at 400 °C for 1 h in air with a heating and cooling rate of 2 °C/min in a muffle oven. To enable THz measurements, the nanotube layers were transferred onto fused silica substrates. The bottom (closed) parts of the nanotube layers were thusly in direct contact with silica substrates.

In order to obtain information about the electronic properties of the nanotube layers (amorphous as well as crystalline), photocurrent measurements were carried out and evaluated. The measurements were performed in an

aqueous electrolyte containing 0.1 M Na_2SO_4, employing a photoelectric spectrophotometer (Instytut Fotonowy), connected with the modular electrochemical system PGSTAT 204 (Metrohm Autolab B.V.), and operated with *Nova 1.10* software. A three-electrode cell with a flat quartz window was employed with a Ag/AgCl reference electrode, a Pt wire counter electrode, and the anodized and annealed Ti substrate as working electrode, pressed against an O-ring of the electrochemical cell leading to an irradiated sample area of 0.28 cm^2. Monochromatic light was provided by a 150 W Xe lamp. The photocurrents were measured at a constant potential of 0.4 V vs. Ag/AgCl in the spectral range from 300 to 500 nm. A shutter of the monochromator was opened for 10 s to obtain a stable plateau of the photocurrent values.

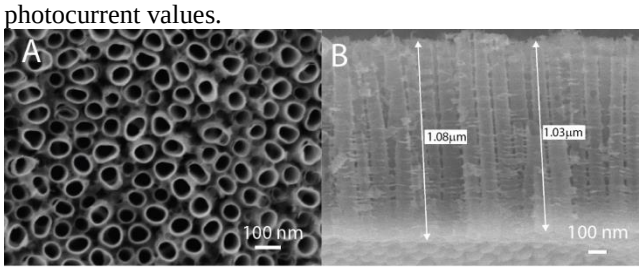

Figure 1 SEM images of self-organized TiO_2 nanotube layer: A) top-view B) cross-section with indicated thickness of the nanotube layers.

The as-anodized amorphous nanotube layers showed a poor performance, namely very low photocurrents, and an incident photon-to-electron conversion efficiency (IPCE), below 5% (Figure 2). The nanotube layers were substantially improved upon by crystallization to the anatase phase: the IPCE then exceeds 60%, and most importantly, the photocurrent density increased. This is in agreement with the expectation that the as-grown amorphous TiO_2 nanotubes provide a high number of structural defects, which lead to recombination of charge carriers before their collection at the electrodes. The annealing step annihilates the structural defects, thus (i) suppressing recombination and (ii) eliminating charge scattering by the defects, thus increasing carrier mobility.

The IPCE of the anatase nanotube layers was approximately constant below ~320 nm, but decreased at longer wavelengths. This behaviour is related to the spectral profile of the anatase absorption coefficient: its absorption lengths are 14 nm, 26 nm, ~50 nm and ~120 nm at the wavelengths 266 nm, 300 nm, 320 and 330 nm, respectively [15]. Using finite-element calculations, it was found that the effective absorption length of the nanotubes is approx. 3 times larger. The shorter wavelengths are thus entirely absorbed by the nanotubes, while the longer-wavelength incident photons pass through the nanotubes as their energy approaches the anatase band gap at 390 nm.

The photoresponse for the wavelengths shorter than ~330 nm is essential for understanding the charge dynamics in the nanotubes. The corresponding photons are fully absorbed in the top part of the nanotubes, therefore the photogenerated charges travel through almost entire nanotube before being collected at the bottom electrode. The observed constant and high IPCE (Figure 2b) then means that these charges do not suffer from substantial recombination despite their long journey. In this situation, if the mobility of charges were time- and position-independent, then also the photocurrent density would be independent of where the charges are generated, i.e., of the excitation wavelength. The observed wavelength dependence of the photocurrent density thus indicates a pronounced dispersion of the mobility, which decreases with increasing transport length. This can be attributed to trapping-detrapping events which the charges encounter during the transport. Importance of trapping-detrapping has been emphasized also in a detailed analysis of the temporal evolution of THz conductivity [13].

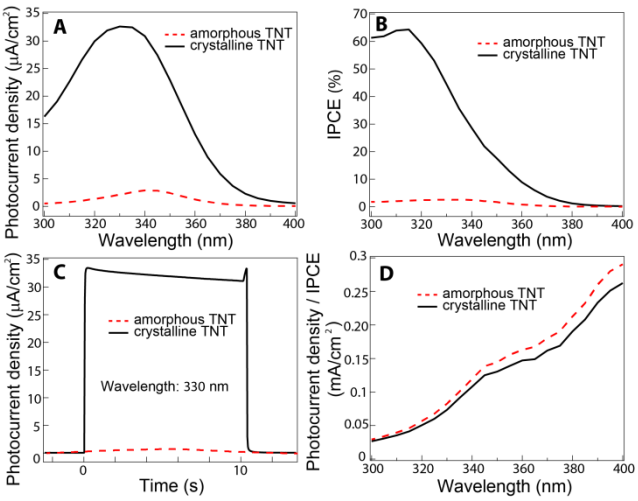

Figure 2 A) photocurrent density B) incident photon-to-electron conversion efficiency C) photocurrent transients recorded and D) ratio of photocurrent density and IPCE for 1 µm thick TiO_2 nanotube layer in amorphous state (red line) and crystalline state (anatase, black line).

To obtain a further insight into the charge transport properties, we employed time-resolved terahertz (THz) spectroscopy [16]. This non-contact technique provides information on charge transport over nanometer distances [17]. The measurements were performed in a common experimental setup driven by a femtosecond Ti:Sapphire laser amplifier (5 kHz repetition rate) described in Ref. [18]. Part of the laser beam was converted to the third harmonics, and the resulting wavelength of 266 nm was used for the photoexcitation of the samples. The pump beam was defocused to ensure the homogeneous generation of photocarriers across the analysed section of the nanotube layers. The experiments were carried out in a low vacuum in order to eliminate the absorption of the THz beam by water vapour.

The THz probe experiment measures the transient THz transmittance spectrum $\Delta E_t/E_t$, where E_t is the spectrum of the THz pulse transmitted through the sample in equilibrium, and ΔE_t is its photo-induced change. Here we briefly summarize the results from Ref. [19] which link the transient transmittance with charge transport properties, characterized by a mobility spectrum. We introduce a normalized transient transmittance

$$\Delta T_{norm} = -\frac{(1+n_s)}{Z_0}\frac{1}{e_0\phi}\frac{\Delta E_t}{E_t}, \qquad (1)$$

where n_s is the refractive index of the substrate, Z_0 is the vacuum impedance, e_0 is the elementary charge and ϕ is the optical excitation fluence expressed in photons/m^2. For samples in the form of thin homogeneous films, ΔT_{norm} is directly equal to the product of the quantum yield of charges and their mobility. This relation is more complicated in inhomogeneous systems, where we first need to establish the relation between the conductivity $\Delta\sigma$ of the TiO_2 (response to the local electric field) and the measured effective conductivity $\Delta\sigma_{eff}$ (response to the electric field of the THz pulse): in Ref. [20], we have shown that

$$\Delta\sigma_{eff} = \Delta\sigma\left(V + \frac{B}{1 + iD\Delta\sigma/(2\pi f\varepsilon_0)}\right). \qquad (2)$$

The coefficients V, B and D reflect the morphology of the sample: the parameters V and B express the fraction of percolated and non-percolated parts, and D is related to the dominant depolarization factor. For known geometries, all coefficients can be determined by calculating the distribution of electric field [19]; for the investigated nanotubes, we found that $V + B \sim 0.15 - 0.23$ (the spread stems from the uncertain degree of connectivity of the nanotubes, as discussed e.g. in Ref. [12]). For the small photoconductivities encountered in TiO_2, the D-term can be neglected, allowing to link ΔT_{norm} to the product of the quantum yield of free charges ξ (considered to be unity shortly after photoexcitation) and their mobility μ [19]:

$$\Delta T_{norm} = (V + B)\frac{\alpha_{loc}}{\alpha}\xi\mu, \qquad (3)$$

where α_{loc} is optical absorption coefficient of TiO_2 and α is the effective absorption coefficient of the nanotube structure. Using finite-element calculations, we obtained $\alpha_{loc}/\alpha \sim 3$. Details of these calculations will be published elsewhere. Note that Eq. (3) is valid only for small transient signals ($\Delta E_t/E_t \ll 1$) [19]; this condition is well satisfied for our samples ($\Delta E_t/E_t$ is on the level of 10^{-3} and 2×10^{-4} for the spectra in Fig. 1, measured for the high and low excitation fluence, respectively). Finally, it should be emphasized that we examined the charge transport in the direction of the probing THz electric field, which is perpendicular to the nanotubes axes.

Figure 3 shows the normalized transient transmittance spectra of the studied samples in amorphous and anatase crystalline state. In both forms, the measured signal does not show a significant dependence on the excitation intensity. This confirms that we are in the regime of weak conductivity where ΔT_{norm} is directly proportional to the mobility of carriers. We thus see that the real part of mobility is slightly increasing with the frequency, whereas the imaginary part is slightly negative (at least for low THz frequencies). These features are typical signatures of carrier confinement.

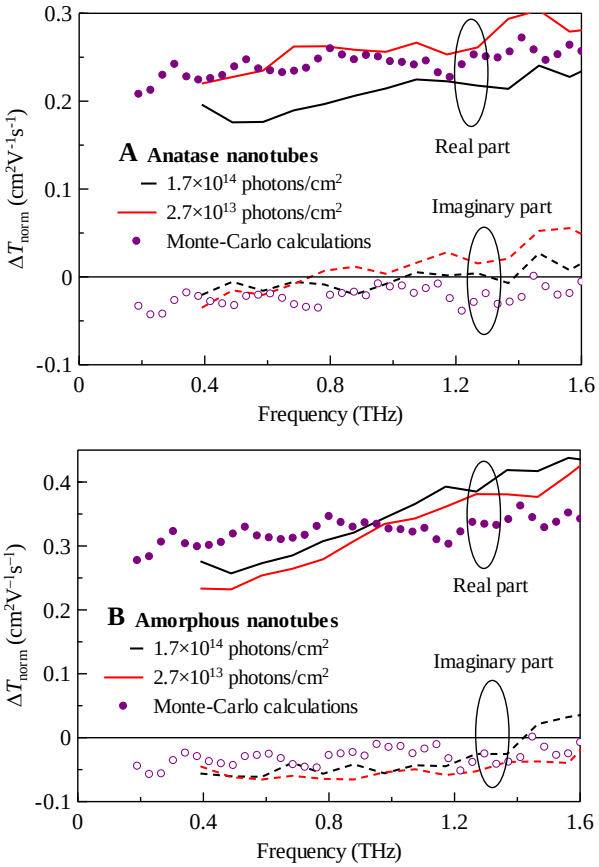

Figure 3 Lines: spectra of normalized transient transmission for the studied A) anatase and B) amorphous samples measured 10 ps after photoexcitation. Symbols: results of Monte-Carlo calculations for $e_0\tau_s/m^* = 0.5$ cm^{2}V^{-1}s^{-1}. Experimental data were obtained for the pump-probe delay of 10 ps. Solid lines and closed symbols: real part, dashed lines and open symbols: imaginary part.

To further understand this behaviour, we employed semi-classical Monte-Carlo calculations of the conductivity of the nanotube layers [21]. This method is based on numerical simulations of thermal trajectories of charges, and on the subsequent calculation of the mobility spectrum using the Kubo formula. We assume that charges (polarons) with effective mass $m^* \sim m_e$ ([22] and references therein) move inside the nanotubes according to the Drude model, with scattering time τ_s. When the carriers reach nanotube boundaries, they are reflected back. In Figure 3, we observe that there is a good match with the measured spectra for $\tau_s = 0.3$ fs, which corresponds to the mobility $e_0\tau_s/m^* = 0.5$ cm^{2}V^{-1}s^{-1} (the accuracy of these values is limited by the uncertainty in the $V + B$ factor). The good match of the shape of the calculated spectrum with the

measured one confirms that charges are indeed confined by the nanotube walls. Effects like band bending [23] should be marginal: if it confined the charges into even smaller volumes, than the shape of the THz spectra would be considerably different [21].

The mobility value is comparable to that observed in anatase nanoparticles [24] and in mesoporous anatase structures [20], but it is considerably lower than the mobility encountered in intrinsic or niobium-doped bulk anatase [25, 26]. We thus conclude that the nanotubes contain a large density of defects responsible for the strong scattering, and that there is still a potential for improving the crystallinity and the transport properties of the nanotubes. Note that the reported scattering time corresponds to a mean free path of ~0.035 Å, which is too short to be compatible with the Drude behaviour. In this sense, the values of τ_s and corresponding mobility should be regarded with a great care. Nevertheless, it is considered that they at least roughly characterize the efficiency of the charge transport in the nanotubes.

Quite surprisingly, the normalized transient transmittance is slightly higher in the amorphous nanotubes, as shown in Figure. 3. Although it is not possible to distinguish whether this is due to a higher mobility or due to a slightly better connectivity (higher sum $V + B$), the results clearly show that the THz mobility (which represents charge mobility on nanocsale distances) in amorphous and anatase nanotube layers is comparable. The same conclusion applies also for the ratio of the photocurrent density and IPCE (Fig. 2d), which can be considered as a measure of *dc* mobility. Similar mobilities of crystalline and amorphous phase were observed also in mesoporous TiO_2 [20].

Regarding charge dynamics, shortly after photoexcitation, charge mobilities both in amorphous and anatase nanotubes are similar. Subsequently, trapping of charges occurs, thus reducing their average mobility, as shown in Figure 4. In amorphous nanotube layers, charge recombination is faster than the transport to the electrodes, which results in the low IPCE value. In the crystalline nanotube layers, the charges are continuously trapped and detrapped, which permits their transport through long distances; at the same time, high IPCE can be achieved due to the slower recombination processes. The time-scale for trapping estimated from the decay of THz photoconductivity is ~1 ns in amorphous nanotubes and somewhat longer in the crystalline ones (Figure 4). In the dc photoresponse experiments, the potential $U = 0.4$ V was applied along the distance $l = 1$ μm (length of the nanotubes). If the charges were moving at the THz mobility $\mu = 0.5$ cm^{2}V^{-1}s^{-1}, it would take them $l^2/(\mu U) = 50$ ns to traverse the entire nanotube. The trapping process thus must be faster than this value, i.e., the nanosecond lifetime of THz photoconductivity is consistent also with the dc measurements.

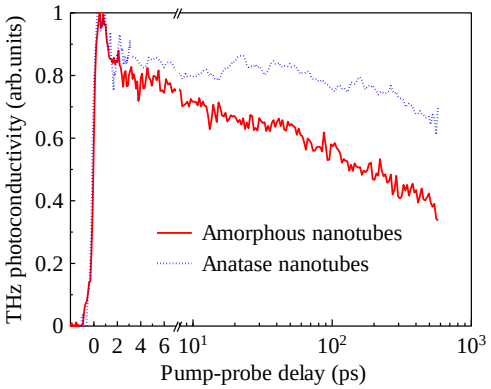

Figure 4 Dynamics of THz photoconductivity (the curves were normalized to the peak value) at 2.7×10^{13} photons/cm^2.

3 Conclusion

Photoelectrochemical measurements and time-resolved terahertz spectroscopy were employed to study charge transport in amorphous and anatase TiO_2 nanotube layers with thickness of 1 μm. The early-time charge mobility in both forms was approximately 0.5 cm^{2}V^{-1}s^{-1}, indicating a potential for further improvement of charge transport properties. Recombination processes substantially decreased the IPCE of amorphous nanotube layers, whereas they were much slower in anatase, allowing a maximum IPCE value, of up to 60%. The *dc* mobility was reduced and controlled by trapping-detrapping of charge carriers.

Acknowledgements European Research Council and Ministery of Youth, Education and Sports of the Czech Republic and Czech Science Foundation are acknowledged for financial support of this work through projects 638857, LM2015082, and 13-12386S, respectively.

References

[1] J. M. Macak, H. Tsuchiya, A. Ghicov, K. Yasuda, R. Hahn, S. Bauer, P. Schmuki, Curr. Opin. Solid State Mater. Sci. **3,** 11(2007)..

[2] K. Lee, A. Mazare, P. Schmuki, *Chem. Rev.* **114**, 9385 (2014). .

[3] K. Zhu, N. Neale, A. Miedaner, A. Frank, Nano Lett.**7**, 69 (2007).

[4] S. So, I. Hwang, P. Schmuki, Energy Environ. Sci. **8**, 849 (2015).

[5] F. Mohammadpour, M. Moradi, K. Lee, G. Cha, S.So, A. Kahnt, D. M. Guldi, M. Altomare and P. Schmuki, Chem. Commun.15, 1631 (2015).

[6] X. Gao, J. Li, J. Baker, Y. Hou, D. Guan, J. Chen and C. Yuan. Chem. Commun. 50, 6368 (2014).

[7] X. Wang, Z. Li, W. Xu, S. A. Kulkarni, S. K. Batabyal, S. Zhang, A. Cao and L. H. Wong, Nano Energy **11**, 728 (2015).

[8] R. Salazar, M. Altomare, K. Lee, J. Tripathy, R. Kirchgeorg, N. T. Nguyen, M. Mokhtar, A. Alshehri, S. A. Al-Thabaiti, P. Schmuki, ChemElectroChem. **2**, 824 **(**2015).

[9] H. Tsuchiya, J. M. Macak, A. Ghicov, A. S. Rader, L. Taveira, P. Schmuki, Corrosion Science **49**, 203 (2007).
[10] A. Ghicov, H. Tsuchiya, J. M. Macak, P. Schmuki, Phys. Stat. Sol. (a) **203,** R28 (2006).
[11] R. Beranek, H. Tsuchiya, T. Sugishima, J. M. Macak, L. Taveira, S. Fujimoto, H. Kisch and P. Schmuki App. Phys. Lett. 87 (2005) 243114-243116.
[12] C. Wehrenfennig, C. M. Palumbiny, H. J. Snaith, M. B. Johnston, L. Schmidt-Mende, and L. M. Herz, J. Phys. Chem. C **119**, 9159 (2015).
[13] C. Richter and C. A. Schmuttenmaer, Nature Nanotech., **5,** 769 (2010)
[14] H. Sopha, L. Hromadko, K. Nechvilova, J.M. Macak, J. Electroanal. Chem., **759,** 122 (2015).
[15] G. E. Jellison, L. A. Boatner, J. D. Budai, B.-S. Jeong, and D. P. Norton, J. Appl. Phys. 93, 9537 (2003).
[16] C. A. Schmuttenmaer, Chem. Rev. **104**, 1759 (2004).
[17] H. Němec, P. Kužel, and V. Sundström, J. Photochem. Photobiol. A **215**, 123 (2010).
[18] L. Fekete, P. Kužel, H. Němec, F. Kadlec, A. Dejneka, J. Stuchlík and A. Fejfar, Phys. Rev. B **79**, 115306 (2009).
[19] P. Kužel and H. Němec, J. Phys. D: Appl. Phys. **47**, 374005 (2014).
[20] H. Němec, V. Zajac, I. Rychetský, D. Fattakhova-Rohlfing, B. Mandlmeier, T. Bein, Z. Mics, and P. Kužel, IEEE T. THz. Science Technol. **3**, 302 (2013).
[21] H. Němec, P. Kužel and V. Sundström, Phys. Rev. B **79**, 115309 (2009).
[22] T. Luttrell, S. Halpegamage, J. Tao, A. Kramer, E. Sutter, and M. Batzill, Sci. Rep. **4**, 4043 (2014).
[23] J. Lloyd-Hughes, S. K. E. Merchant, L. Sirbu, I. M. Tiginyanu, and M. B. Johnston, Phys. Rev. B 78, 085320 (2008).
[24] S. A. Jensen, K.-J. Tielrooij, E. Hendry, M. Bonn, I. Rychetský, and H. Němec, J. Phys. Chem. C **118**, (2014).
[25] L. Forro, O. Chauvet, D. Emin, L. Zuppiroli, H. Berger, and F. Lévy, J. Appl. Phys. **75**, 633 (1994).
[26] Y. Furubayashi, T. Hitosugi, Y. Yamamoto, K. Inaba, G. Kinoda, Y. Hirose, T. Shimada, and T. Hasegawa, Appl. Phys. Lett. **86**, 252101 (2005).